

# Nanorobot Locomotion by Breaking the Scallop Theorem

Joshua Merz<sup>1</sup> and Isaac Torres-Diaz<sup>2</sup>

<sup>1</sup>Depart. of Electrical & Computer Eng., <sup>2</sup>Depart. of Chemical & Materials Eng.

## Motivation

**Applications:** Nanorobots are relevant in medicine for drug delivery, minimally invasive surgery, and other biomedical applications.

**Problem:** Robots lose actuation and directed locomotion for smaller scales, such as at nanoscale.

**Challenge:** How to make nanorobots with multiple actuation.

## Methodology

**The Scallop Theorem** dictates that at Low Reynolds numbers, time symmetric movements (like the swimming scallop fig. 4) generate no net propulsion.

**Breaking the Scallop Theorem.** We designed simple magnetic nanorobots modeled as a Rauss Bead-Spring model with three spheres connected by Hookean springs (fig. 5) dictated by  $\mathbf{F}_s = -k\Delta\mathbf{x}$ . We then exposed these robots to time-varying magnetic fields.

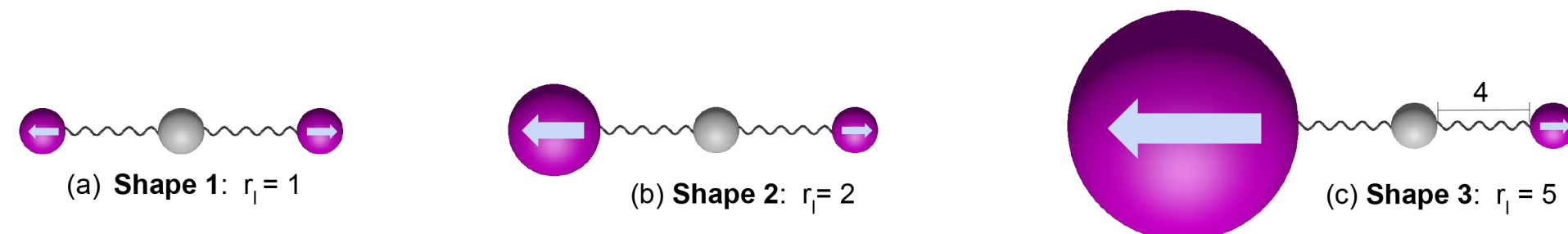


Figure 5: Three particle systems connected by Hookean springs of length 4 and dimensionless parameter  $k = 3$ . The arrows denote the permanent magnetic moments on the particles, which are proportional to particle volume. Leftmost sphere radii ( $r_i$ ) labeled on (a) shape 1, (b) shape 2, and (c) shape 3.

**Brownian Dynamics Simulations:** Particles translation and rotational movements in a fluid are described by the Langevin Equation

$$\Delta\mathbf{x} = \mathbf{M}_{UF} \cdot \mathbf{F}_{ext} \Delta t + \mathbf{X}_B, \quad (1)$$

$$\Delta\Phi = \mathbf{M}_{\omega T} \cdot \mathbf{T}_{ext} \Delta t + \mathbf{W}_B. \quad (2)$$

Inertia becomes negligible and motion is determined by magnetic, hydrodynamics, and Brownian forces and torques.

**Simulation Overview:** We expose the magnetic robots to time-varying magnetic fields with different particle-field interaction parameter ( $\alpha$ ). We track the robot configuration in time with respect to its initial position and orientation (figs. 5-7).

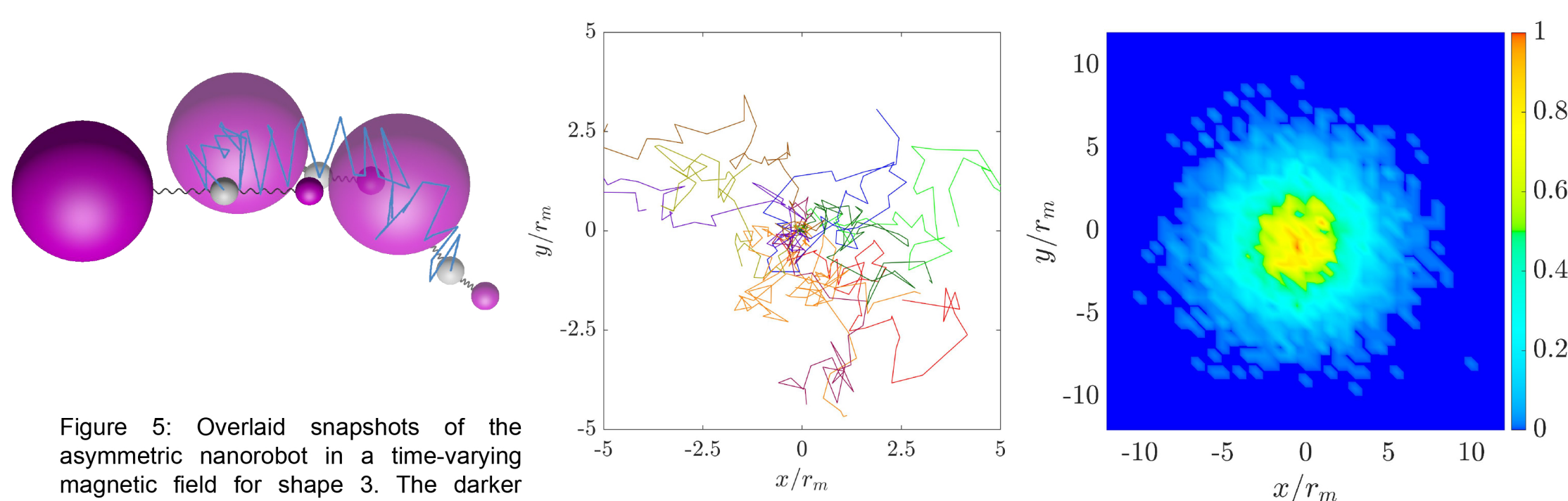


Figure 5: Overlaid snapshots of the asymmetric nanorobot in a time-varying magnetic field for shape 3. The darker color nanorobot represents the starting configuration. The faded colors represent the time steps at  $t=25$  and  $t=50$ . The blue line represents the nanorobot trajectory.

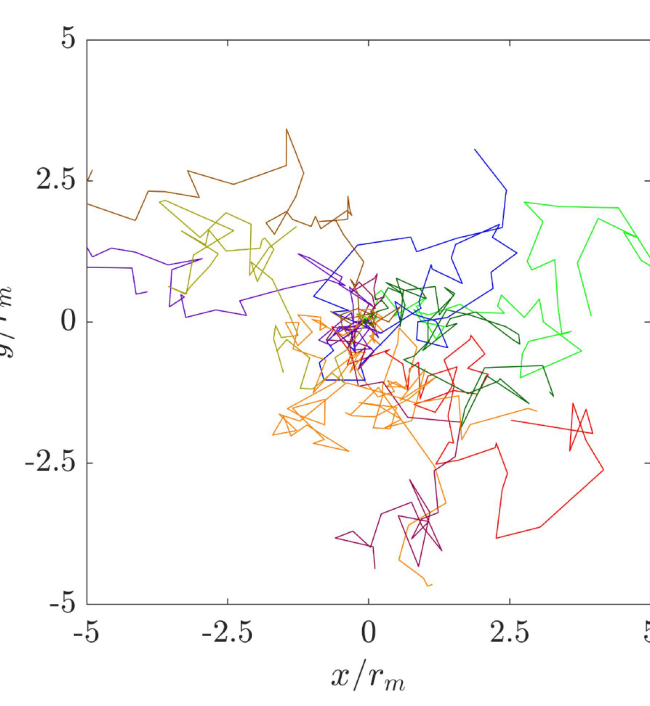


Figure 6: Nanorobot center of mass trajectories for different simulations in time for shape 3.

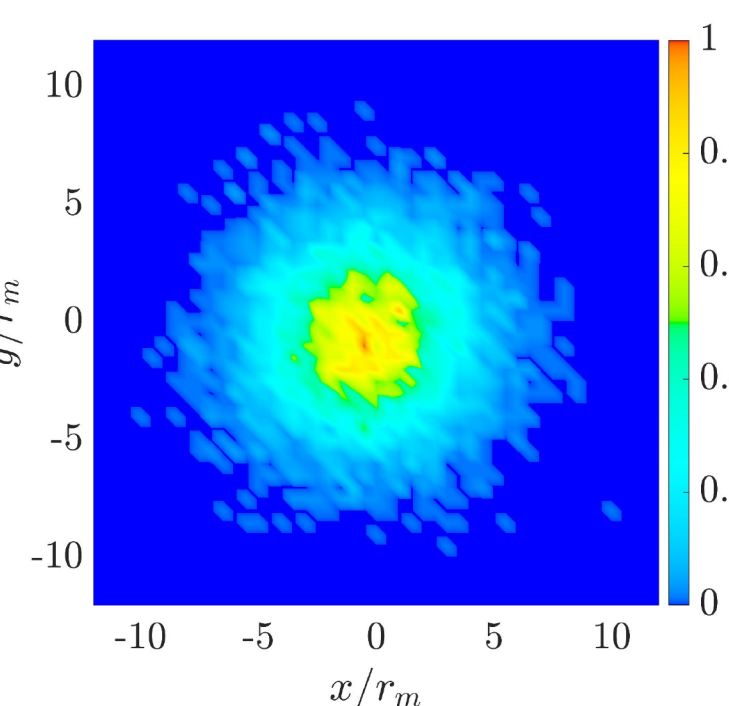


Figure 7: Probability distribution of the final nanorobot (shape 3) position after  $t = 50$ .

## References

1. L. Turner, W.S. Ryu, H.C. Berg. "Real-Time Imaging of Fluorescent Flagellar Filaments." *Bacteriol* 182, 2793 (2000).
2. H. Xu, M. Medina-Sánchez, V. Magdanz, L. Schwarz, F. Hebenstreit, O.G. Schmidt. "Sperm-Hybrid Micromotor for Targeted Drug Delivery." *ACS Nano* 12, 1, 327-337 (2018).
3. M. Wehner, R. Truby, D. Fitzgerald, B. Mosedegh, G. Whitesides, J. Lewis, R. Wood. "An integrated design and fabrication strategy for entirely soft, autonomous robots." *Nature* 536, 451-455 (2016).

## Acknowledgements

All RCEU projects were sponsored in part by the Alabama Space Grant Consortium, the UAH Office of the President, Office of the Provost, Office of the Vice President for Research and Economic Development, the Deans of the College of Science, the College of Engineering, the College of Arts, Humanities, and Social Sciences, the College of Education, and the College of Nursing. Nanorobot configurations in fig. 1 generated from data provided by David Harris.

## Results

We analyze the final center of mass of the nanorobots and generate the probability distributions for different configurations (Shapes 1, 2, and 3) and particle-field interaction parameter ( $\alpha = 0, 3$ , and  $10$ ).

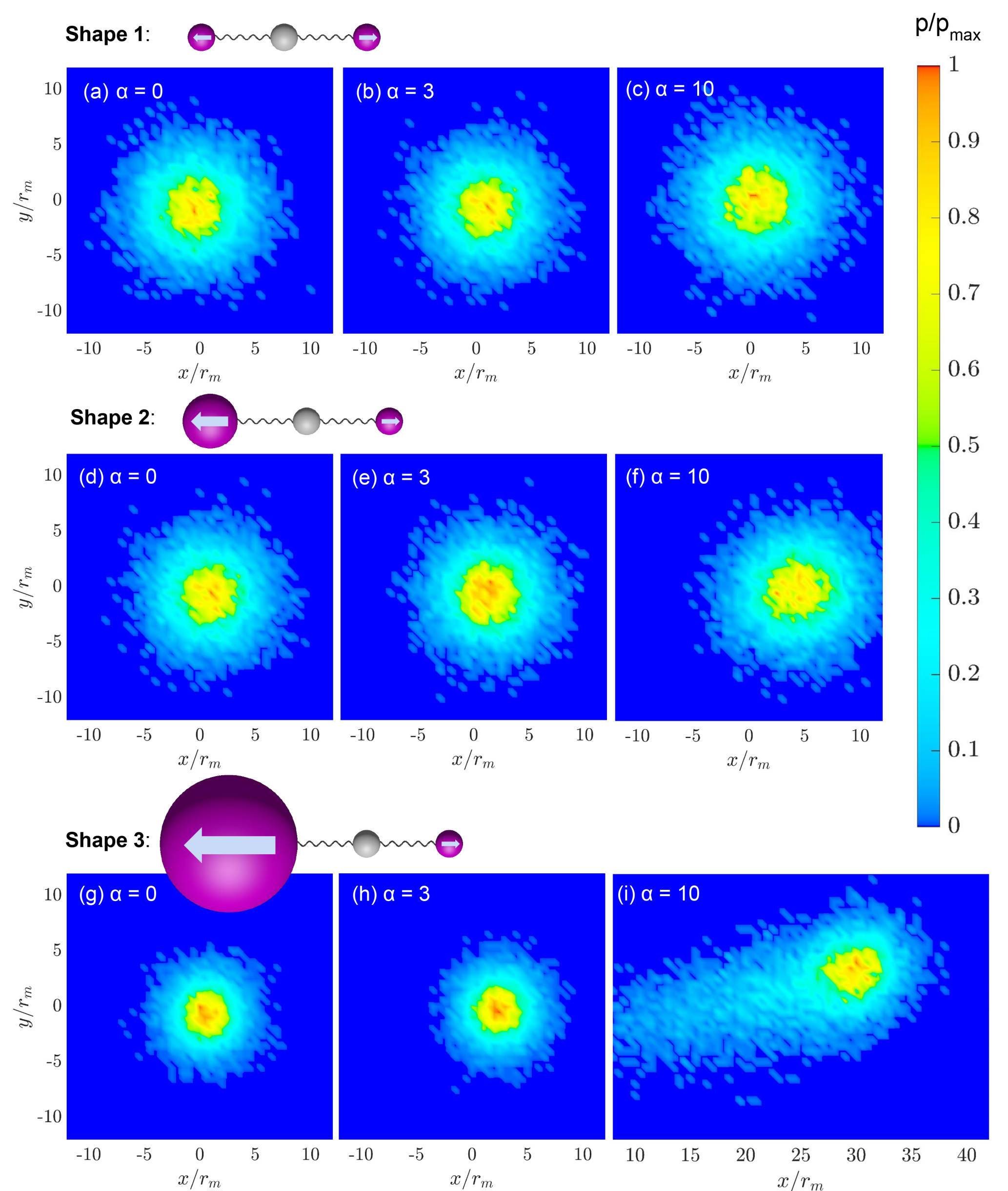


Figure 6: Probability distribution of the final nanorobot position after  $t = 50$  for different  $\alpha$  values in (a)-(c) shape 1, (d)-(f) shape 2, and (g)-(i) shape 3. As the particle-field interaction parameter  $\alpha$  increases and the robot's symmetry is broken the displacement increases.

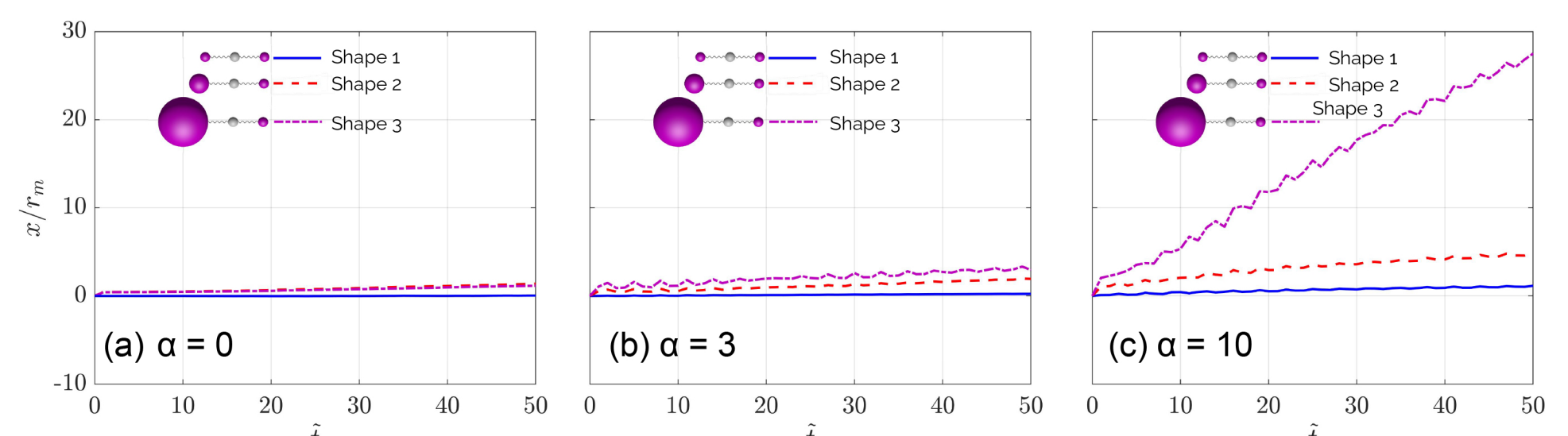


Figure 9: Mean displacement in the  $x$  direction of the shapes across 10,000 trials as a function of time for different particle-field parameters (a)  $\alpha=0$ , (b)  $\alpha=3$ , and (c)  $\alpha=10$ . The displacement of shapes 2 (b) and 3 (c) in a time-varying magnetic fields increases due to symmetry breaking of the nanorobot.

## Conclusions and Future Work

We show that breaking the symmetry of a three-particles linked nanorobot in a time-varying field generates a net propulsion. Moving forward, we aim to study different particle shapes (ellipsoids), and utilize asymmetries to generate propulsion and other actuations in 3D nanorobots (fig. 10).

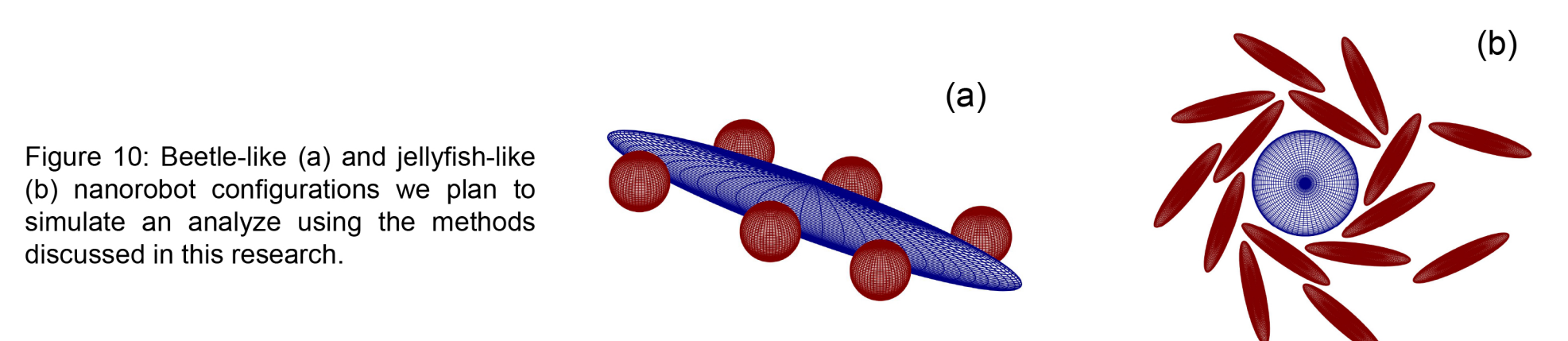


Figure 10: Beetle-like (a) and jellyfish-like (b) nanorobot configurations we plan to simulate and analyze using the methods discussed in this research.